A Mouse Model of Human Hyperinsulinism Produced by the E1506K Mutation in the Sulphonylurea Receptor SUR1

Kenju Shimomura,[1] Maija Tusa,[2] Michaela Iberl,[1] Melissa F. Brereton,[1] Stephan Kaizik,[1] Peter Proks,[1] Carolina Lahmann,[1] Nagendra Yaluri,[2] Shalem Modi,[2] Hanna Huopio,[3] Jarkko Ustinov,[4] Timo Otonkoski,[4,5] Markku Laakso,[2] and Frances M. Ashcroft[1]

Loss-of-function mutations in the K_{ATP} channel genes *KCNJ11* and *ABCC8* cause neonatal hyperinsulinism in humans. Dominantly inherited mutations cause less severe disease, which may progress to glucose intolerance and diabetes in later life (e.g., SUR1-E1506K). We generated a mouse expressing SUR1-E1506K in place of SUR1. K_{ATP} channel inhibition by MgATP was enhanced in both homozygous (homE1506K) and heterozygous (hetE1506K) mutant mice, due to impaired channel activation by MgADP. As a consequence, mutant β-cells showed less on-cell K_{ATP} channel activity and fired action potentials in glucose-free solution. HomE1506K mice exhibited enhanced insulin secretion and lower fasting blood glucose within 8 weeks of birth, but reduced insulin secretion and impaired glucose tolerance at 6 months of age. These changes correlated with a lower insulin content; unlike wild-type or hetE1506K mice, insulin content did not increase with age in homE1506K mice. There was no difference in the number and size of islets or β-cells in the three types of mice, or evidence of β-cell proliferation. We conclude that the gradual development of glucose intolerance in patients with the SUR1-E1506K mutation might, as in the mouse model, result from impaired insulin secretion due a failure of insulin content to increase with age. ***Diabetes* 62:3797–3806, 2013**

Congenital hyperinsulinism of infancy (HI) is a rare genetic disorder characterized by enhanced insulin secretion that leads to persistent hypoglycemia soon after birth (1,2). It occurs in ~1 in 50,000 live births within the general population and at higher levels in communities that practice consanguineous marriage. The severity of the disease varies from a mild form, which responds to treatment with drugs (such as diazoxide or octreotide), to a severe drug-resistant form, which may require removal of most of the pancreas. Early diagnosis is important to avoid irreversible brain damage due to the hypoglycemia. Loss-of-function mutations in either the pore-forming (Kir6.2, encoded by *KCNJ11*) or regulatory (SUR1, *ABCC8*) subunit of the β-cell plasma membrane ATP-sensitive potassium (K_{ATP}) channel are the most common causes of HI (3–6).

The K_{ATP} channel plays a crucial role in insulin secretion by coupling the energy state of the β-cell to the plasma membrane potential (5). It achieves this by sensing changes in intracellular adenine nucleotides, being inhibited by ATP binding to Kir6.2 and activated by MgATP (and MgADP) binding and hydrolysis at the nucleotide-binding domains of SUR1 (7,8). As a consequence, the K_{ATP} channel is open when metabolism is low, keeping the β-cell membrane hyperpolarized and preventing insulin secretion. An increase in β-cell metabolism, consequent on elevation of the plasma glucose concentration, leads to an increase in intracellular ATP and K_{ATP} channel closure. This produces a membrane depolarization that opens voltage-gated Ca^{2+} channels, stimulating Ca^{2+} influx and exocytosis of insulin granules. Loss-of-function mutations in either Kir6.2 or SUR1 result in permanent membrane depolarization, persistent Ca^{2+} influx, and thus continuous, unregulated insulin release (2–6).

Most reported mutations in *KCNJ11* and *ABCC8* that cause HI are inherited recessively; these mutations cause the most severe form of the disease. However, a few dominantly expressed mutations have also been described (9–15). Children with these mutations generally have a milder phenotype than those with recessive mutations, and their hypoglycemia is well controlled by the K_{ATP} channel opener diazoxide. Members of one family, who are heterozygous carriers of the SUR1-E1506K mutation, have mild neonatal HI but are at increased risk of diabetes in middle age (9,14); 4 out of 11 had overt diabetes, and 5 of those without diabetes showed impaired glucose tolerance. Similarly, a child with a heterozygous SUR1-R370S mutation causing neonatal hyperinsulinism developed diabetes at 10 years of age (15). Studies of other dominantly inherited mutations have not shown a link between HI mutations and late-onset diabetes, although the disease severity may diminish later in life as many patients no longer require diazoxide therapy and become normoglycemic (12).

Despite their impaired glucose tolerance, blood glucose levels were normal in heterozygous carriers of the SUR1-E1506K mutation without diabetes, and only slightly increased in those with diabetes (14). Electrophysiological studies indicate that the E1506K mutation does not impair membrane trafficking but results in channels that are no longer activated by MgATP (9,16). As a consequence, homozygous whole-cell K_{ATP} currents are absent, and heterozygous K_{ATP} currents are 30–50% smaller than wild type

From the [1]Henry Wellcome Centre for Gene Function, Department of Physiology, Anatomy and Genetics, University of Oxford, Oxford, U.K.; the [2]Department of Medicine, University of Eastern Finland and Kuopio University Hospital, Kuopio, Finland; the [3]Department of Pediatrics, University of Eastern Finland and Kuopio University Hospital, Kuopio, Finland; the [4]Research Programs Unit, Molecular Neurology, Biomedicum Stem Cell Centre, University of Helsinki, Helsinki, Finland; and the [5]Children's Hospital, Helsinki University Central Hospital, Helsinki, Finland.

Corresponding author: Frances M. Ashcroft, frances.ashcroft@dpag.ox.ac.uk.

Received 20 November 2012 and accepted 24 July 2013.

DOI: 10.2337/db12-1611

This article contains Supplementary Data online at http://diabetes.diabetesjournals.org/lookup/suppl/doi:10.2337/db12-1611/-/DC1.

K.S., M.T., M.I., and M.F.B. contributed equally to this study.

(WT). The smaller K_{ATP} currents would be expected to result in membrane depolarization, thus accounting for the increased insulin secretion in human neonates. Why this translates into reduced insulin secretion later in life is unclear, as is why impaired insulin secretion was observed in all carriers of the E1506K mutation but diabetes in only some of them.

Unexpectedly, genetic deletion of SUR1 in mice did not mimic human hyperinsulinism (6,17–20). $SUR1^{-/-}$ mice exhibited hypoglycemia on the first day of life but normal blood glucose levels subsequently (17), and by 12 weeks of age, they showed impaired glucose tolerance (17,18). The β-cell resting membrane potential was depolarized (17), and the basal intracellular calcium concentration was elevated (18), as expected if K_{ATP} channels were blocked. Reported data on insulin secretion from $SUR1^{-/-}$ islets are controversial. Early studies suggested that basal insulin secretion was not elevated (17) and that glucose-induced insulin secretion from isolated islets (17) and perfused pancreas (18) was severely impaired. However, subsequent studies showed that basal insulin secretion is elevated (as expected from the raised $[Ca^{2+}]_i$), that after overnight culture in 10 mmol/L glucose, glucose-stimulated insulin release is greater than from WT islets (19,20), and that the amplifying effect of glucose on insulin secretion is intact. What remains unclear, however, is why $SUR1^{-/-}$ mice have a different phenotype from the human disease, and why some human mutations cause diabetes later in life.

To address these questions, we generated a mouse carrying a human HI mutation, SUR1-E1506K, which causes neonatal hypoglycemia and predisposes to diabetes late in life (9,14). We show here that both homozygous and heterozygous mice secrete more insulin than their WT littermates early in life, but with age, homozygous mice secrete less insulin and become increasingly glucose intolerant.

RESEARCH DESIGN AND METHODS

Generation of E1506K mice. Knock-in mice expressing the murine SUR1 (*Abcc8*) gene containing a G-to-A missense mutation corresponding to the human SUR1-E1506K mutation were produced by targeted mutagenesis. The genomic sequence homologous to the human SUR1 locus 1506 was identified using basic local alignment search tools (BLAST) for nucleotide and protein. The GAA-to-AAA change, corresponding to the GAG-to-AAG mutation in human SUR1-E1506K carriers, was introduced into mouse genomic DNA spanning 8.6 kb over the *Abcc8* gene exons 30–39. (Note that the human L78208 *ABCC8* isoform encodes 1,582 amino acids and contains an additional residue in NBD1; consequently, E1506 in our sequence is equivalent to E1507 [16]). A neomycin resistance gene, flanked by 109-bp-long LoxP fragments, was introduced in the middle of intron 36. An additional FseI restriction site was inserted in intron 37 to facilitate cloning.

The targeting vector (Fig. 1*A*) was introduced into 129SVPas embryonic stem (ES) cells by electroporation. Transfected cells were identified by neomycin selection, and ES cell clones that had undergone homologous recombination were confirmed by Southern blotting. The selected ES cells were microinjected into C56BL/6 blastocysts to produce chimeric mice. Chimeric mice were bred with mice expressing Cre recombinase to generate offspring in which the neo cassette was excised. These mice were then back-crossed to C57Bl/6J mice to segregate the *cre* transgene, and $Sur1^{wt/E1506K}/neo^{-/-}/cre^{-/-}$ offspring were used for further breeding. Transgenic pups were identified by PCR. The presence of the G-to-A nucleotide change was verified by sequencing the mutated gene region.

Animal care. Experiments were conducted in accordance with the U.K. Animals Scientific Procedures Act (1986) and University of Oxford ethical guidelines. Mice were housed in a temperature- and humidity-controlled room on a 12-h light-dark cycle. Regular chow food containing 63% carbohydrate, 23% protein, and 4% fat (RM3; Special Diet Services) was freely available except when mice were fasted. Mice had ad libitum access to water.

Western blotting. Islets were isolated and pooled from 3-month-old male mice of the same genotype, and Western blotting was performed on three samples per genotype. Proteins were extracted using RIPA buffer plus protease and phosphatase inhibitors (Roche). Lysates were centrifuged at 13,000*g* for 30 min, and the supernatant was collected and kept at −70°C until further analysis. Protein concentrations were measured using a BCA protein assay kit (Thermo Scientific, Waltham, MA). Proteins (20 μg/lane) were loaded onto Novex Nupage Bis-Tris 4–12% gels (Invitrogen), subjected to gel electrophoresis, and transferred to polyvinylidene fluoride membranes. For immunoblotting of SUR1, membranes were blocked in 5% BSA and 0.1% TBS-Tween for 1 h at room temperature (RT) and incubated with primary antibody (1:1,000 in blocking buffer; Santa Cruz Biotechnology, Santa Cruz, CA) at 4°C overnight. The secondary antibody was donkey anti-goat IgG-HRP (incubated 1:10,000 in blocking buffer for 1 h at RT; Santa Cruz Biotechnology). For α-tubulin, membranes were blocked in 3% milk plus 0.05% PBS-Tween for 1 h and incubated with primary antibody (Sigma-Aldrich) at a dilution of 1:10,000 in blocking buffer for 1 h and then with secondary anti-mouse horseradish peroxidase–conjugated immunoglobulin (1:20,000 in blocking buffer; GE Healthcare) for 1 h; all incubations were conducted at RT. Membranes were washed with 0.05% PBS-Tween for 3 times every 5 min after blocking, primary antibody incubation, and also after antibody incubation. Bands were visualized using chemiluminescence (ECL plus; GE Healthcare), captured using an Image Quant RT-ECL machine (version 1.0.1; GE Healthcare), and quantified using Quantity One software (Bio-Rad). SUR1 protein expression was normalized to α-tubulin protein levels.

Quantitative immunohistochemistry. Pancreata were isolated from WT or homE1506K mice 2 (3 + 3), 6 (4 + 4), or 12 months of age (5 + 6) and serially sectioned, and five 3-μm sections were collected every 100 μm. Deparaffinized and rehydrated sections were treated with 1 mmol/L EDTA buffer (pH 8) to reveal antigen sites, incubated for 10 min in in Ultra V Block (Thermo Scientific) to block nonspecific binding sites, and incubated overnight at 4°C with insulin (guinea pig anti-swine; DakoCytomation) or Ki67 (rabbit anti-human; Novocastra, Newcastle upon Tyne, U.K.) antibody. For insulin staining, sections were incubated for 30 min at RT with a biotinylated secondary antibody (Zymed Laboratories, San Francisco, CA), rinsed, incubated with peroxidase-conjugated streptavidin (Zymed Laboratories), and developed with 3-amino-9-ethyl-carbazole substrate (Thermo Scientific). For Ki67 staining, the secondary antibody was donkey anti-rabbit IgG (Alexa, A21206; Invitrogen, Carlsbad, CA). Nuclei were stained with DAPI (Vector Laboratories, Burlingame, CA). Morphometric analysis was performed using an Image-Pro Analyzer 6.0 (Media Cybernetics, Bethesda, MD).

Quantitative PCR. Total RNA was extracted from ~100 isolated islets using the RNeasy Lipid Tissue Mini Kit (Qiagen) with an on-column DNase digestion step to remove genomic DNA. RNA concentration was determined in triplicate using a NanoDrop ND-1000 spectrophotometer (Thermo Scientific) and quality checked with an Agilent Bioanalyzer. Equal quantities of total RNA were reverse transcribed using the High Capacity cDNA Reverse Transcription Kit (Applied Biosystems). An equal amount of total RNA was processed identically but without reverse transcriptase (non-RT control). The reaction cycle consisted of a 10-min incubation at 25°C followed by a 30-min incubation at 48°C.

Quantitative PCR was performed using an ABI Prism 7000 sequence detection system (Applied Biosystems) and SYBR Green reagents (Power SYBR Green; Applied Biosystems). Primers were designed using Geneious Pro software (Biomatters, Inc.) based on National Center for Biotechnology Information sequence data (for sequences see reference 21). Each reaction consisted of 20 ng cDNA, 12.5 μL 2× Power SYBR Green master mix, 300 nmol/L primers (forward and reverse), and nuclease-free water (final volume of 25 μL). The reaction cycle comprised an initial denaturation for 10 min at 95°C, followed by 40 cycles of 95°C/15 s and 60°C/60 s. All reactions were performed in triplicate. Non-RT controls were included in each experiment. The ABI 7000 SDS software (Applied Biosystems) was used to measure threshold cycle (Ct) values. Gene expression was determined using the Pfaffl method (22) and normalized to three housekeeping genes: *ACTB*, *HPRT1*, and *HSPA8*.

Glucose tolerance tests. Mice were fasted overnight, and a fasted blood sample was taken prior to intraperitoneal (intraperitoneal glucose tolerance test [IPGTT]) administration of a 2 g/kg glucose load. Subsequent blood samples were taken over time from a tail vein under local anesthesia (5% EMLA cream; AstraZeneca) for glucose measurement. In some experiments, free-fed plasma glucose levels were measured daily (at 2:00 P.M.). Plasma glucose was measured using a FreeStyle Lite Blood Glucose Monitoring System (Abbott).

For plasma insulin measurements, mice were fasted overnight and killed 30 min after an intraperitoneal glucose injection (2 g/kg glucose). Whole blood was collected from the vena cava, and plasma was separated for insulin measurements using a Mercodia mouse ELISA kit.

Insulin secretion. Mice were killed by cervical dislocation, the pancreas was removed, and islets were isolated by liberase digestion and handpicking, as previously described (23). Islets were cultured overnight in RPMI solution

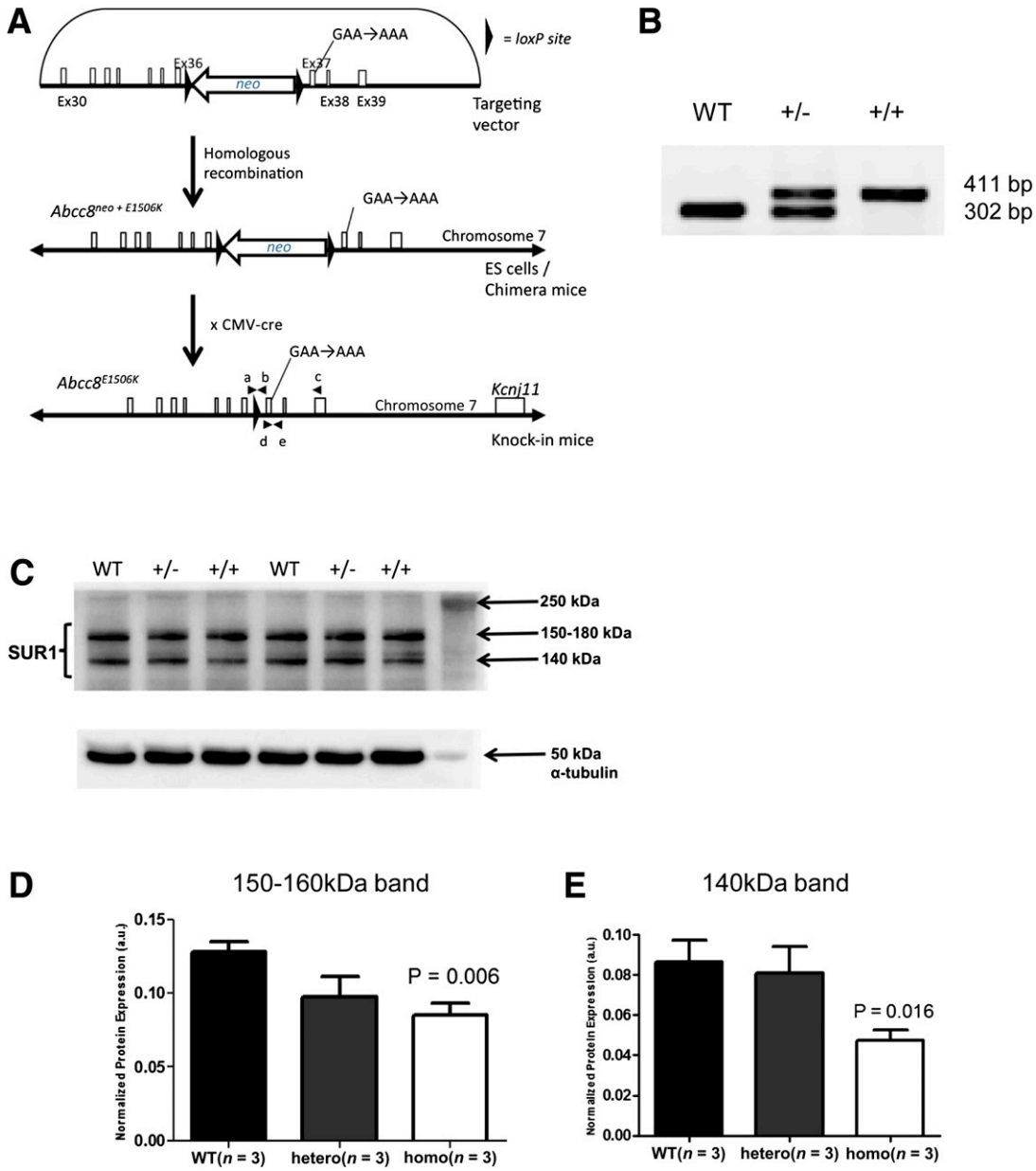

FIG. 1. Targeted mutagenesis of the murine *Abcc8* gene and production of the SUR1-E1506K knock-in mice. *A*: The mutated *Abcc8* sequence was introduced into ES cells by homologous recombination, and the ES cells were microinjected into C56BL/6 blastocysts to produce chimeric mice. Chimeric mice were first crossbred with *cre* mice to excise the neo cassette, and then back-crossed to C57Bl/6J to segregate the *cre* transgene. The $Abcc8^{w/E1506K}/neo^{-/-}/cre^{-/-}$ offspring were used for further breeding. *B*: Transgenic pups were identified by PCR from ear lysates using primers a and b (shown in *A*). The knock-in pups yielded a longer PCR product due to the 109-bp LoxP site remaining in the DNA after the Cre recombination. The presence of the G to A nucleotide change in the mice was verified by amplifying the DNA and sequencing the PCR product. *C*: Western blots of SUR1 and α-tubulin protein expression in islets isolated from 3-month-old mice ($n = 3$). The two SUR1 bands (at 140 and 150–180 kDa) likely represent immature and mature glycosylated protein, respectively. *D* and *E*: Mean ± SEM SUR1 protein levels, normalized to α-tubulin, for islets isolated from WT, hetE1506K, and homoE1506K mice ($n = 3$ in each case). *D*: 150–180 kDa. *E*: 140-kDa protein. *P* values indicate the comparison between WT and homE1506K (ANOVA); other comparisons between the two groups (homE1506K vs. hetE1506K; hetE1506K vs. WT) were not statistically significant.

containing 5 mmol/L glucose (Gibco), supplemented with 100 units/mL penicillin and 100 μg/mL streptomycin, at 37°C in a humidified atmosphere of 5% CO_2/95% air. After overnight culture, insulin secretion was measured from islets perifused at 37°C and a rate of 1 mL · min^{-1} with Krebs-Ringer-HEPES buffer (in mmol/L): 120 NaCl, 4.7 KCl, 2.5 $CaCl_2$, 1 KH_2PO_4, 1.2 $MgSO_4$, 10 HEPES, and 25 $NaHCO_3$, pH 7.4 (with NaOH), plus 0.1% BSA and glucose and tolbutamide as indicated (23). A 0.5 mol/L stock solution of tolbutamide was made in DMSO and diluted as required. After 30 min preperifusion in 2 mmol/L glucose, the perifusate was collected every 1 min. At the end of the experiment, islets were incubated overnight at −20°C with acidified ethanol solution (95% ethanol, 5% acetic acid) to extract all insulin. Insulin was measured using a Mercodia mouse ELISA kit.

Electrophysiology. Islets were dissociated into single cells using calcium-free Hanks' solution (1 mmol/L EGTA) (23). Currents were recorded from cell-attached (at 0 mV) or inside-out membrane patches (at −60 mV), filtered at 5 kHz, and digitized at 20 kHz. The pipette contained (mmol/L) 140 KCl, 10 HEPES (pH 7.2 with KOH), 1.1 $MgCl_2$, and 2.6 $CaCl_2$. The intracellular (bath) solution contained (in mmol/L) 107 KCl, 1 $CaCl_2$, 2 $MgCl_2$, 11 EGTA, and 10 HEPES (pH 7.2 with KOH), plus MgATP as indicated. Concentration-response curves were fit with Eq. 1: $I/I_c = 1/(1 + ([ATP]/IC_{50})^h)$, where I and I_c are the current amplitudes in the presence and absence of ATP, IC_{50} is the ATP concentration at which inhibition is half maximal, and h is the slope factor. To control for current rundown in excised patches, I_c was taken as the mean of the conductance in control solution before and after ATP application.

Calcium measurements. Isolated islets were loaded with 3 μmol/L Fura-2 AM (Invitrogen) for 20 min at RT in EC buffer plus 0.01% pluronic acid (137 mmol/L NaCl, 5.6 mmol/L KCl, 1.2 mmol/L $MgCl_2$, 2.6 mmol/L $CaCl_2$, and 10 mmol/L HEPES, pH 7.4 with NaOH). Individual islets were then transferred to a perfusion chamber mounted on the stage of an Axiovert 200 microscope (Zeiss), held in place by a glass suction pipette, and perfused with EC buffer plus 2 mmol/L glucose at 33–35°C for 15 min prior to the start of the experiment. Glucose and tolbutamide were then perfused as indicated. Changes in $[Ca^{2+}]_i$ were recorded using a ratiometric fluorescence system (Photon Technology International) with dual excitation at 340 and 380 nm and emission at 510 nm. Images were acquired at two frames per second. Ca^{2+} signals are presented as the ratio of signal recorded with different excitation wavelengths (F340/F380). Data were analyzed using FeliX32 Analysis software. Basal $[Ca^{2+}]_i$ in 2 mmol/L glucose was measured as the average signal during an ~14-min application. The peak calcium responses were measured as the average signal for ~30 s around the maximal value.

Statistics. Data are mean ± SEM. Significance was tested with Student *t* test unless otherwise stated.

RESULTS

Generation of SUR1-E1506K mice. Mice homozygously expressing the E1506K mutation in SUR1 were generated by targeted mutagenesis of the SUR1 (*Abcc8*) gene (Fig. 1*A*) and back-crossed for eight generations onto a C57BL/6J background. Genotyping demonstrated the presence of the mutant allele in heterozygous SUR1-E1506K (hetE1506K) and homozygous E1506K (homE1506K) mice (Fig. 1*B*). C57BL/6J mice were used as controls and to generate heterozygous E1506K mice.

Western blotting suggested that SUR1 protein levels were significantly lower in homE1506K islets than WT islets when normalized to tubulin (Fig. 1*C–E*). No reduction in SUR1 mRNA expression was observed with quantitative PCR in islets from 6-month-old mice (Supplementary Fig. 1).

Morphometry revealed that islet density was similar in the three groups of mice (Fig. 2*A*), and quantitative analysis showed no difference in the relative cross-sectional area of the pancreas occupied by islets, or in individual islet size, between WT and homE1506K mice, at 2, 6, or 12 months of age (Table 1). At 2 months of age, mean β-cell size was slightly larger in homE1506K than WT islets, but there was no difference at 6 or 12 months. β-Cell proliferation, measured by Ki67 and insulin double immunoreactivity, was similar in WT and homE1506K mice (Fig. 2*B* and Table 1). Human HI islets are also normal in number size and general appearance (24).

Electrophysiology. There was no significant difference in K_{ATP} current density, measured as the peak current after patch excision, between β-cells isolated from WT, hetE1506K, and homE15906K mice at 2 months of age (Fig. 3*A* and Supplementary Fig. 2). However, a significant reduction in K_{ATP} channel activity was seen in 6-month-old homE1506K β-cells.

The E1506K mutation increased the sensitivity of the K_{ATP} channel to MgATP, half-maximal inhibition being produced by 33, 14, and 10 μmol/L in inside-out patches from WT, hetE1506K, and homE1506K β-cells, respectively (Fig. 3*B* and Supplementary Table 1). These values are similar to those reported for WT β-cells (25 μmol/L) (23), and for WT (28 μmol/L) (25) and homE1506K channels (9.3 μmol/L) (9) when expressed in *Xenopus* oocytes. The small increase in block is attributable to the reduction in Mg nucleotide–mediated activation produced by the mutation (Fig. 3*C*). These data also show that, as suggested from studies of heterologously expressed channels (9), mutant SUR1-E1506K subunits do not exert a dominant-negative effect on WT subunits in vivo. There was no change in ATP sensitivity of homE1506K K_{ATP} channels with age (Supplementary Fig. 3).

We measured the number of cells that showed action currents (reflecting action potential activity) and K_{ATP} channel activity in cell-attached patches. No action potential activity was observed in WT cells, and 75% of patches

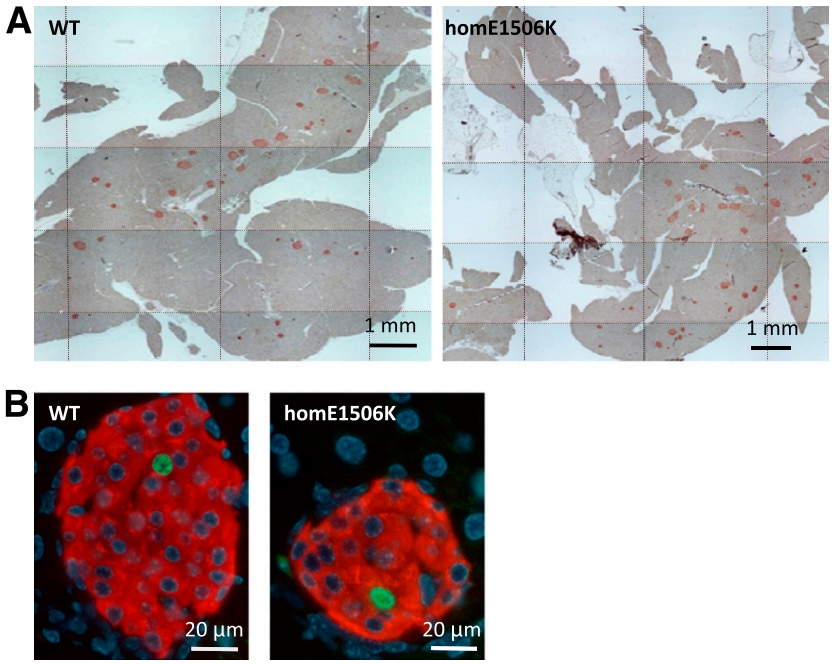

FIG. 2. ***A*: Sections of pancreas from WT (*left*) and homE1506K (*right*) 3-month-old mice used for morphometric analysis. Islets are immunostained with anti-insulin (red). Composite figures of multiple adjacent fields are shown. *B*: Double immunofluorescent staining for insulin (red) and Ki67 (green, for detection of proliferating β-cells) in WT (*left*) and homE1506K (*right*) mice.**

TABLE 1
Morphometric analysis of pancreatic islets in WT and homE1506K mice

	2 months		6 months		12 months	
	WT	homE1506K	WT	homE1506K	WT	homE1506K
Islet area (% whole pancreas)	0.37 ± 0.10	0.47 ± 0.13	0.32 ± 0.20	0.38 ± 0.12	0.60 ± 0.16	0.62 ± 0.18
Mean islet size (μm^2)	3,300 ± 400	4,600 ± 300	4,000 ± 2,100	3,900 ± 1,300	8,100 ± 2,000	7,300 ± 1,800
Mean β-cell size (μm^2 ins area/cell)	144 ± 3	167 ± 4**	136 ± 3	132 ± 6	159 ± 8	164 ± 6
β-Cell proliferation (INS+Ki67 positive cells/mm^2 ins area)	34 ± 7	34 ± 7	8.8 ± 2.1	11.5 ± 7.1	19 ± 8	17 ± 5

**$P < 0.01$ against WT (Student t test); ins area, insulin-staining area.

showed K_{ATP} channel activity (Fig. 3*D* and Supplementary Table 1). In contrast, 63% of homE1506K patches had action currents and only 13% had K_{ATP} channel activity, consistent with the increased sensitivity of the channel to MgATP inhibition.

Intracellular calcium measurements. In 2-month-old WT islets, intracellular calcium $[Ca^{2+}]_i$ increased when glucose was elevated from 2 to 10 mmol/L and showed a further small increase on subsequent addition of the K_{ATP} channel blocker tolbutamide (Supplementary Fig. 4*A*). HetE1506K islets generated some spontaneous Ca^{2+} oscillations in 2 mmol/L (basal) glucose (Supplementary Fig. 4*B*), due to the presence of electrical activity. However, the average $[Ca^{2+}]_i$ in 2 mmol/L glucose was similar to that of WT islets, and increased when glucose was raised (Supplementary Fig. 4*F*). Basal $[Ca^{2+}]_i$ was elevated in

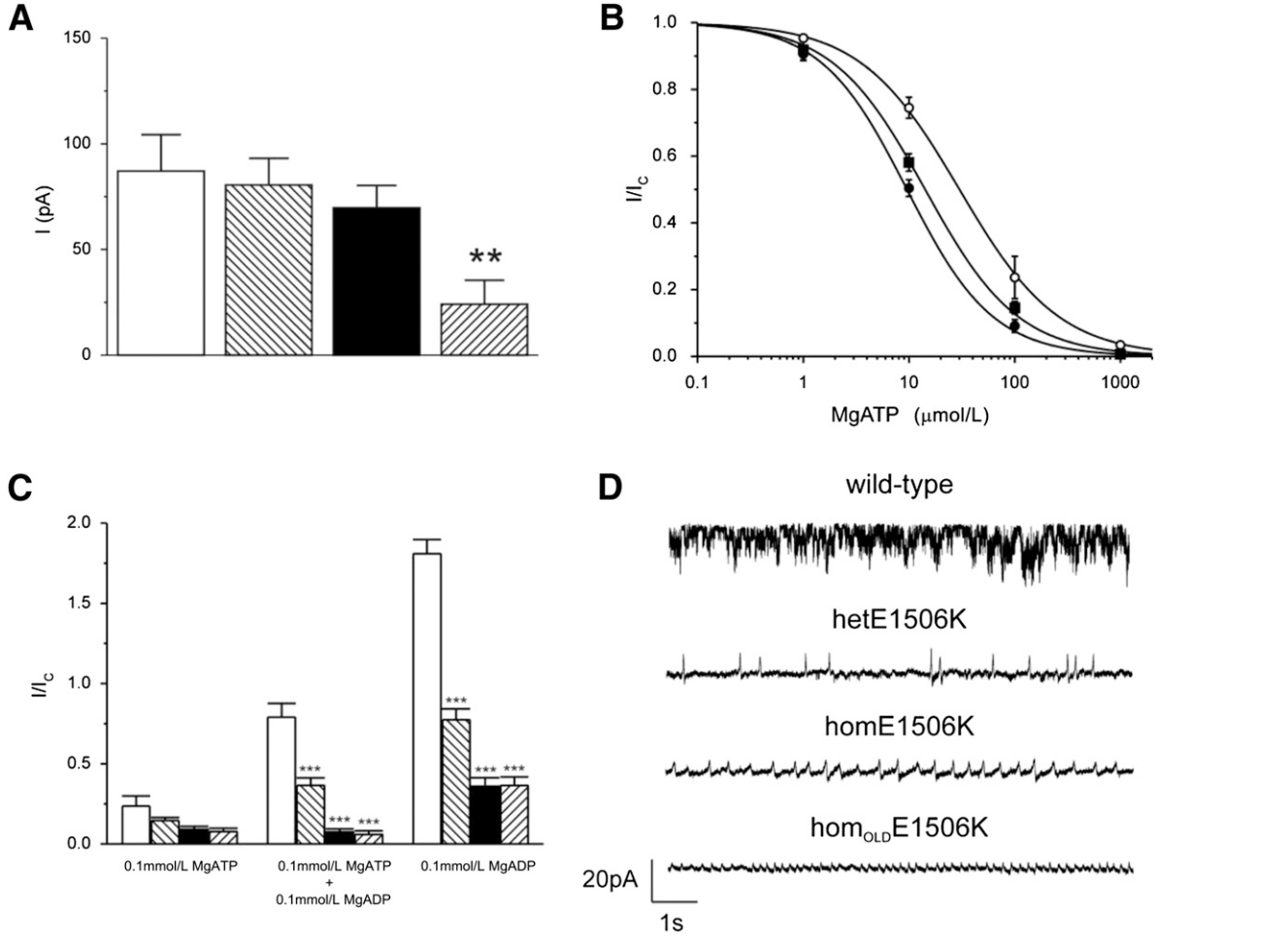

FIG. 3. ***A*: Mean peak K_{ATP} current values recorded at −60 mV upon patch excision into ATP-free solution from 2-month-old WT (white bar, $n = 20$, 2 mice), hetE1506K (*left* diagonal bar, $n = 30$, 3 mice), and homE1506K (black bar, $n = 30$, 3 mice) β-cells and from 6-month-old homE1506K β-cells (*right* diagonal bar, $n = 30$, 3 mice). **$P < 0.01$ against WT. *B*: Mean ± SEM MgATP concentration-inhibition relationships for K_{ATP} currents recorded from β-cells isolated from 2-month-old WT (open circles, $n = 6$ patches, 3 mice), hetE1506K (black squares, $n = 7$ patches, 3 mice), and homE1506K (black circles, $n = 7$ patches, 3 mice) mice. Current (I) is expressed relative to that in ATP-free solution (I_c). The curves are the best fit of Eq. 1 to the mean data with $IC_{50} = 29$ μmol/L and $h = 0.93$ (WT), $IC_{50} = 14$ μmol/L and $h = 0.99$ (hetE1506K), and $IC_{50} = 9.6$ μmol/L and $h = 1.1$ (homE1506K). *C*: Mean ± SEM currents recorded from WT (white bar, $n = 7$), hetE1506K (*left* diagonal bar, $n = 7$), and homE1506K (black bar, $n = 7$) 2-month-old mice, and 6-month-old homE1506K mice (*right* diagonal bar, $n = 7$), in the presence of 0.1 mmol/L MgATP, 0.1 mmol/L MgADP, or 0.1 mmol/L MgATP plus 0.1 mmol/L MgADP. ***$P < 0.001$ against WT. *D*: Representative examples of on-cell recordings from WT, hetE1506K, and homE1506K β-cells. The spikes are action currents.**

homE1506K islets, reflecting increased electrical activity (Supplementary Fig. 4*C* and *F*), and addition of 10 mmol/L glucose led to a fall in $[Ca^{2+}]_i$, due to stimulation of Ca^{2+} extrusion and/or uptake into stores. In contrast to WT and hetE1506K islets, average $[Ca^{2+}]_i$ in homE1506K islets was not different in 2 and 10 mmol/L glucose. Essentially similar results were obtained at 6 months of age (Supplementary Fig. 5).

Physiological studies. There was no difference in body weight between WT, hetE1506K, and homE1506K mice at 2 or 6 months of age (Supplementary Fig. 6). There was also no significant difference in insulin sensitivity, even at 12 months of age (Supplementary Fig. 7).

At 2 months of age there were no significant differences in fasting plasma glucose levels between WT, hetE1506K, and homE1506K mice, which were 4.3 ± 0.3 (n = 71), 4.1 ± 0.3 (n = 8), and 3.4 ± 0.3 mmol/L (n = 11), respectively (Fig. 4*A*). Free-fed blood glucose levels were slightly higher in homE1506K mice (Supplementary Fig. 8*A*). Plasma glucose levels during an IPGTT were not significantly different between WT, hetE1506K, and homE1506K mice (Fig. 4*A*). However, there was a trend for glucose to take longer to return to control levels in homE1506K mice. Insulin levels, measured 30 min after glucose injection, were not significantly different in WT, hetE1506K, and homE1506K mice (Supplementary Fig. 8*B*).

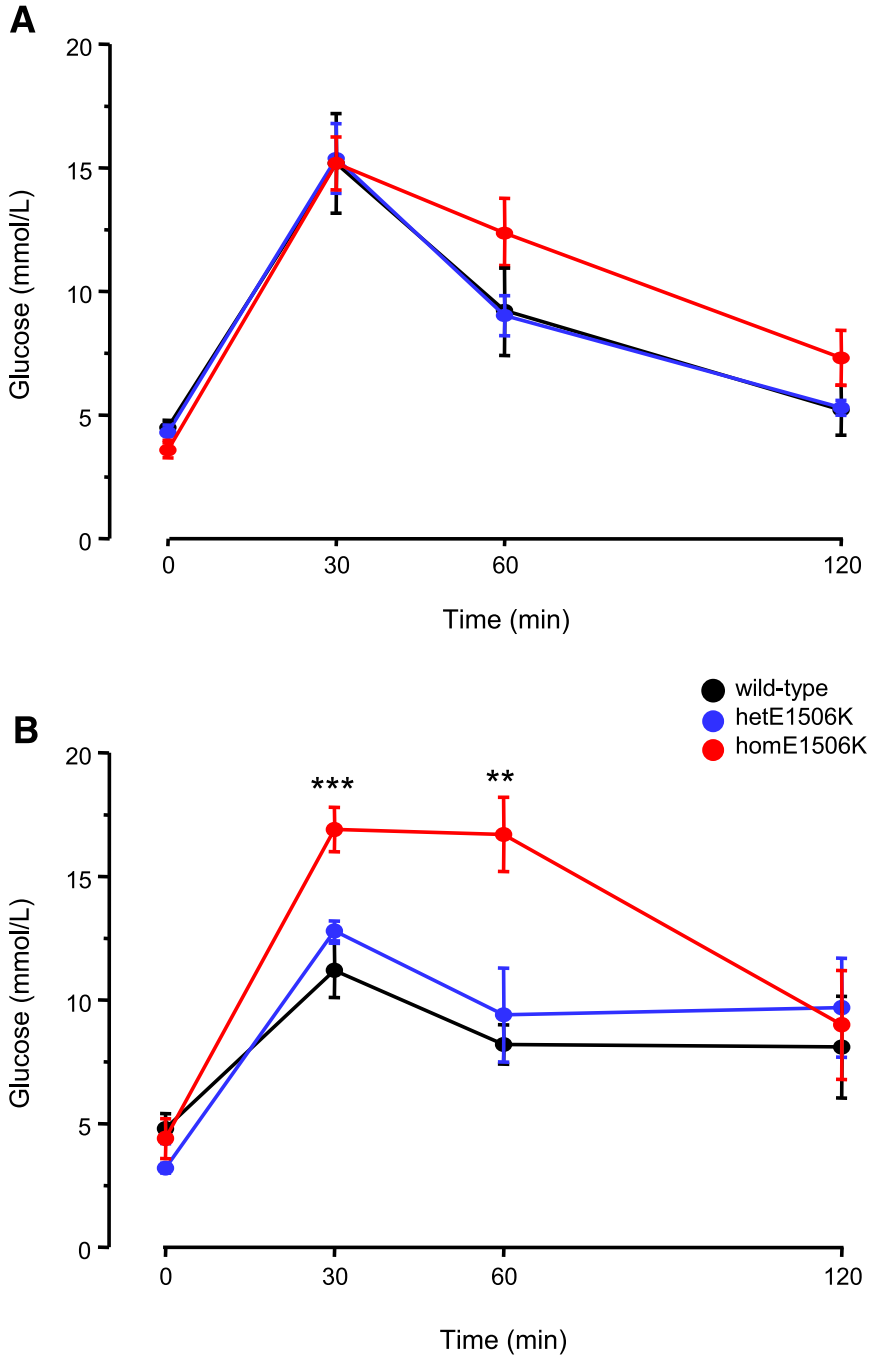

FIG. 4. Plasma glucose levels measured in an intraperitoneal glucose tolerance test in WT (open circles, n = 11 mice), hetE1506K (blue circles, n = 8), or homE1506K (red circles, n = 7 mice) at 2 (*A*) and 6 months of age (*B*). ***P < 0.001 against WT; **P < 0.01 against WT (Student t test).

At 6 months of age, the fasting plasma glucose concentration was 4.8 ± 0.6 (n = 5), 3.2 ± 0.2 (n = 5), and 4.4 ± 0.8 mmol/L (n = 8) for WT, hetE1506K, and homE1506K mice, respectively. Similar plasma glucose levels were reached in WT and hetE1506K mice during an IPGTT, but homE1506K mice were much less glucose tolerant, and significantly so at the 30 and 60-min time points (Fig. 4*B*).

Insulin secretion. At 2 months of age, islets isolated from WT mice showed low basal secretion (at 2 mmol/L glucose) and a clear biphasic increase in insulin secretion at 10 mmol/L glucose (Fig. 5*A*). Addition of tolbutamide further increased insulin secretion. There was no difference in basal secretion in hetE1506K islets, but both first- and second-phase insulin secretion in response to 10 mmol/L glucose were elevated. Tolbutamide had a small effect on insulin secretion but not as marked as in WT islets.

As expected, if their K_{ATP} channels were dysfunctional and basal intracellular calcium was elevated, 2-month-old homE1506K islets had enhanced insulin secretion in 2 mmol/L glucose (Fig. 5*A*). HomE1506K islets also exhibited an enhanced response to 10 mmol/L glucose, and, as predicted, there was no effect of tolbutamide. Qualitatively similar results were obtained if data were expressed in terms of insulin content rather than the absolute amount of insulin secreted (Fig. 5*B*).

WT islets secreted substantially more insulin in response to either 10 mmol/L glucose or tolbutamide, when isolated from 6-month-old mice than from 2-month-old mice (compare Fig. 5*A* and *C*). Consequently, the difference in glucose-stimulated insulin secretion between WT and hetE1506K islets was less at 6 months of age, although second-phase secretion had a tendency to be slightly higher in hetE1506K islets (Fig. 5*C*). More dramatically, glucose was no longer more effective at simulating secretion from homE1506K islets than WT or hetE1506K islets. Indeed, at least for first-phase secretion, it was significantly less effective (Fig. 5*C*). Tolbutamide enhanced secretion from hetE1506K islets, but less than from WT islets. As expected, homE1506K islets did not respond to tolbutamide. Interestingly, insulin secretion increased with age in both WT and hetE1506K islets but not in homE1506K mice.

An altogether different picture was seen when insulin secretion was normalized to insulin content (Fig. 5*D*). In this case, there was little difference in glucose-stimulated insulin secretion from WT, hetE15096K, and homE1506K islets. However, homE1506K islets showed a substantially higher basal level of insulin secretion, consistent with their elevated $[Ca^{2+}]_i$ (Supplementary Fig. 5*C–F*).

These data can be explained by differences in insulin content (Fig. 6*A*). At 2 months of age, insulin content was not significantly different in WT and hetE1506K islets and only ~35% smaller in homE1506K islets. By 6 months of age, insulin content had approximately doubled in both WT islets and hetE1506K islets, but there was little

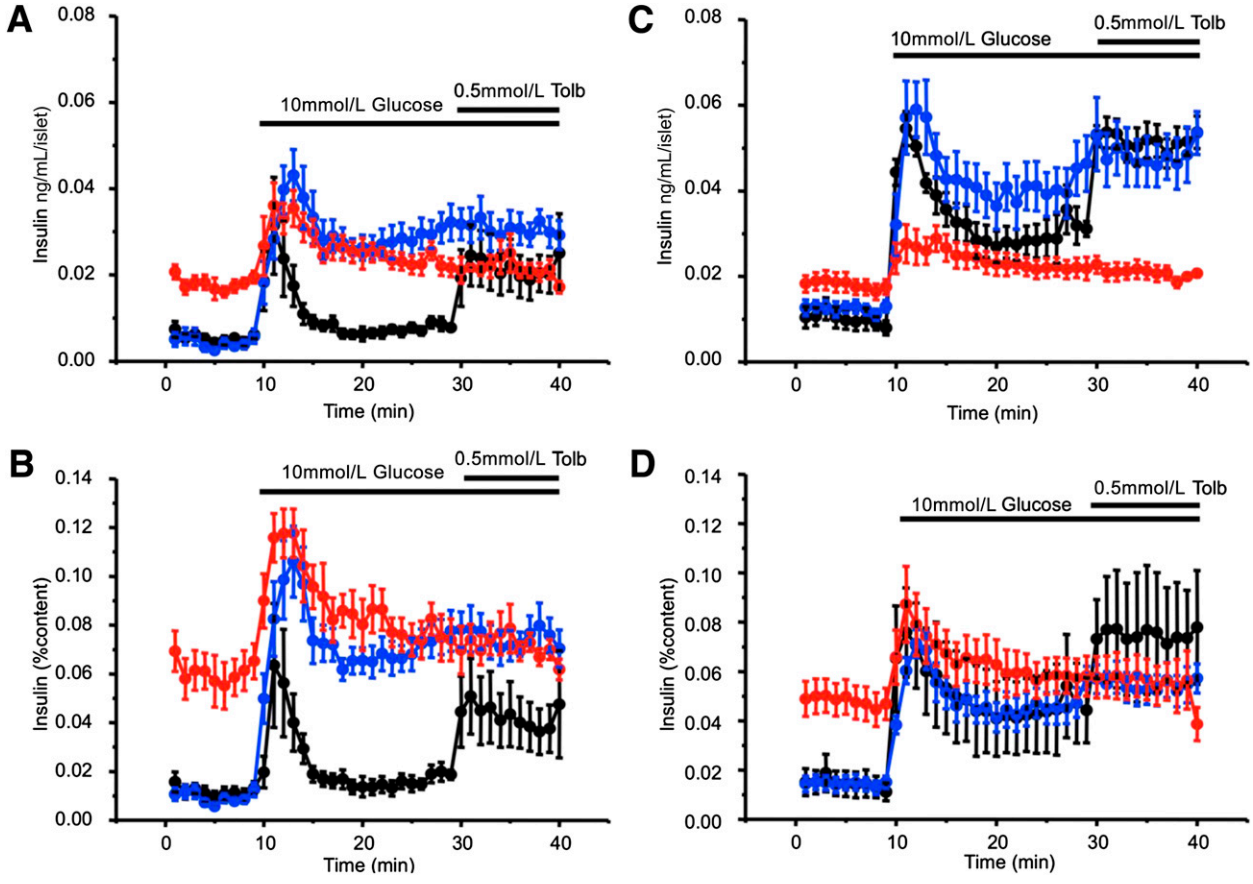

FIG. 5. Insulin secretion from perifused islets in response to 2 mmol/L glucose, 10 mmol/L glucose, or 10 mmol/L glucose and 0.5 mmol/L tolbutamide (Tolb). Islets were isolated from mice aged 2 (*A* and *C*) or 6 months (*B* and *D*). Data are expressed as total insulin secreted (*A* and *C*) or as a percentage of insulin content (*B* and *D*). *A* and *C*: WT (black, n = 5 mice), hetE1506K (blue, n = 5), and homE1506K (red, n = 5 mice). *B* and *D*: WT (black, n = 5 mice), hetE1506K (blue, n = 7), and homE1506K (red, n = 11 mice).

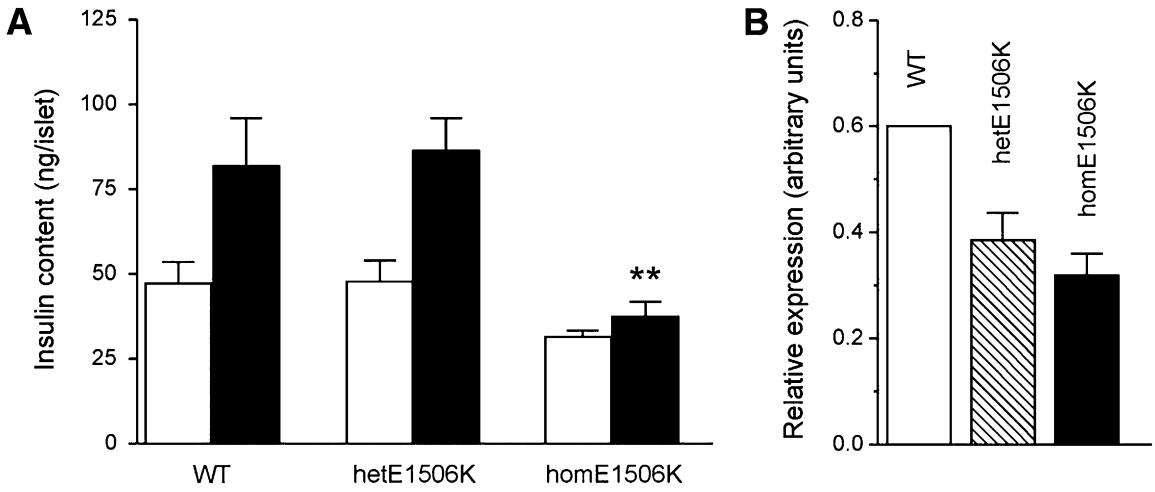

FIG. 6. ***A*****: Insulin content measured at 2 (white bars) and 6 months of age (black bars) in islets isolated from WT (2 months, $n = 4$; 6 months, $n = 5$ mice), hetE1506K (2 months, $n = 4$; 6 months, $n = 5$ mice), and homE1506K (2 months, $n = 4$; 6 months, $n = 5$ mice).** ***B*****: Quantitative PCR of insulin mRNA measured in islets isolated from 6-month-old WT ($n = 2$), hetE1506K ($n = 4$), and homE1506K ($n = 4$) mice. $P < 0.01$ against WT (6 months of age) and hetE1506K (6 months of age). $^{**}P < 0.01$ against WT. Student t test.**

increase in homE1506K islets. Insulin gene expression was also less in islets from 6-month-old homE1506K mice (Fig. 6*B*). There was no obvious difference in the size or number of islets that could be isolated from 6-month-old WT, hetE1506K, and homE1506K mice, consistent with the morphometric data analysis.

DISCUSSION

Effects at 2 months of age. At 2 months of age, islets isolated from homE1506K mice showed elevated basal insulin secretion (at 2 mmol/L glucose), resembling that found for SUR1$^{-/-}$ islets (17) and WT islets in the presence of K_{ATP} channel blockers (26). This is because their K_{ATP} channels are more ATP sensitive and are closed at basal glucose levels; thus their β-cells persistently generate action potentials, leading to elevated $[Ca^{2+}]_i$. The greater basal insulin secretion is consistent with the slightly lower fasting blood glucose levels of homE1506K mice compared with WT mice. Basal insulin secretion, and fasting blood glucose, was unchanged in 2-month old hetE1506K islets, presumably because on-cell K_{ATP} channel activity was only slightly less than for WT β-cells.

The marked increase in secretion from homE1506K islets produced by increasing glucose from 2 to 10 mmol/L was not accompanied by a rise in $[Ca^{2+}]_i$ and is therefore mediated by events downstream of $[Ca^{2+}]_i$ elevation. This confirms that the metabolic amplifying pathway (26) is functionally intact in homE1506K mice, as it is in SUR1$^{-/-}$ mice (19,20). Interestingly, WT islets secreted less insulin (as a percentage of insulin content) in response to 10 mmol/L glucose than either homE1506K or hetE1506K islets. One possible explanation for this finding is that 10 mmol/L glucose is not sufficient to fully close K_{ATP} channels in WT islets, so that the amplifying effects of glucose are not fully enabled.

Despite the enhanced insulin secretion from isolated islets at 2 months of age, fed plasma insulin levels were not significantly different, there was no clear effect of the mutation on glucose tolerance (as measured by an IPGTT), and mice did not become hypoglycemic. This is similar to what is found for SUR1$^{-/-}$ mice (17) and suggests that changes in other tissues may compensate for the enhanced insulin secretion, such as impaired incretin pathways (27) or increased insulin sensitivity. However, insulin sensitivity was unaltered (as found for SUR1$^{-/-}$ mice) (17), which favors the former idea. Similarly, some patients heterozygous for the E1506K mutation have severely reduced insulin secretion but no overt diabetes or glucose intolerance (9,14).

It is noteworthy that the MgATP sensitivity of hetE1506K and homE1506K channels is not very different, yet there is a marked difference in on-cell K_{ATP} channel activity and action potential firing. It is possible that this relates to the stimulatory effect of MgADP in the presence of MgATP, which was substantially greater for hetE1506K channels.

In addition to closing K_{ATP} channels, sulphonylureas bind to Epac2 and stimulate insulin secretion downstream of K_{ATP} channel closure (28). We therefore predicted that tolbutamide might still stimulate insulin exocytosis in homE1506K mice. However, this was not observed. Tolbutamide also did not stimulate secretion from SUR1$^{-/-}$ islets (20). Taken together, this suggests that sulphonylurea stimulation of insulin secretion via Epac2 may require the presence not only of SUR1 but also of a functional K_{ATP} channel.

Effects at 6 months of age. By the age of 6 months, homE1506K islets secreted slightly more insulin in the basal state than WT islets, and much less insulin in response to glucose. This explains why mutant mice have normal fasting blood glucose levels but are significantly less tolerant of a glucose challenge than WT mice. However, when plotted as a function of insulin content, basal insulin secretion was significantly greater than either WT or hetE1506K islets, and the amplifying effect of insulin secretion was intact. Our data thus argue that the reduced insulin secretion that develops with age arises because of lower insulin content in older homE1506K islets. Indeed, the insulin content of homE1506K mice does not change with age whereas that of WT and hetE1506K mice approximately doubles. Levels of insulin mRNA in 6-month-old homE1506K islets are also half those in WT mice.

It is not possible to say whether the lower insulin content is the cause, or a secondary consequence, of the glucose intolerance; or if the two are intimately linked with one driving the other in a vicious cycle. Although chronic

exposure to high glucose can lead to downregulation of insulin gene transcription, much higher glucose levels (33 mmol/L) (29) were needed than those seen in homE1506K mice subjected to a glucose challenge. At lower levels, glucose stimulates insulin gene transcription (30). It is possible that the enhanced basal insulin secretion caused by the E1506K mutation, which necessitates increased insulin production to maintain the same insulin content, places an additional stress on the β-cell that eventually leads to impaired insulin synthesis and/or trafficking (31). Alternatively, long-term elevation of intracellular calcium may ultimately lead to reduced insulin production. Interestingly, in vitro studies have shown that chronic exposure to glibenclamide (which simulates the effect of the E1506K mutation) also reduces insulin content (32).

Comparison with other mouse models. In mice, deletion of Kir6.2 or SUR1 does not cause sustained hypoglycemia as it does in humans; instead, blood glucose levels normalize within a few days of birth, and in later life, animals develop glucose intolerance (17,33). This is also the case for mice homozygous for the Kir6.2-Y12X mutation, which causes recessive hyperinsulinism in humans (34). Although heterozygous Kir6.2 and SUR1 knockout mice show mild hyperinsulinism and improved glucose tolerance (35), mice heterozygous for Kir6.2-Y12X show normal glucose tolerance (34), as is the case for hetE1507K mice. Why there are differences between the different mouse models and the human phenotype is puzzling.

Nichols and colleagues (35,36) have postulated a progressive inverse-U relationship between β-cell excitability and insulin secretion (Fig. 7). In this model, adult $SUR1^{+/-}$ and $Kir6.2^{+/-}$ mice sit on the ascending limb of the relationship and $Kir6.2^{-/-}$ and $SUR1^{-/-}$ mice on its descending limb (35). HomE1506K mice would sit on the ascending limb when 2 months of age and the descending limb at 6 months of age, but hetE1506K mice would remain close to WT at both ages. Although the E1506K mutation is dominant, homE1506K mice mimic the human disease more closely than hetE1506K mice. Why this is the case is unclear but presumably reflects differences in genetic background, lifestyle, or compensatory changes.

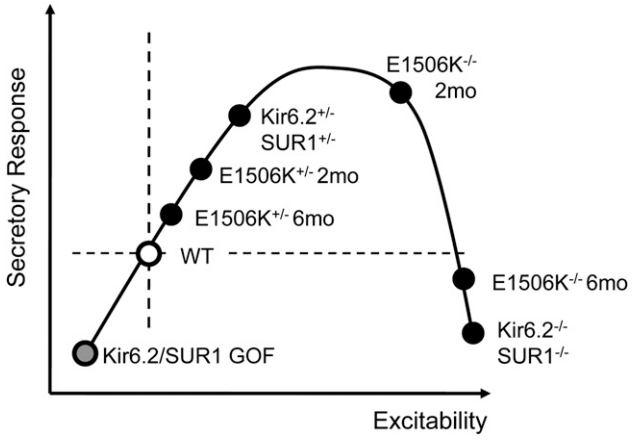

FIG. 7. Relationship between β-cell excitability and glucose-induced insulin secretion (after reference 31). WT islets show the normal secretory response to glucose. Gain-of-function mutations in Kir6.2 or SUR1 (Kir6.2/SUR1 GOF) reduce excitability and insulin secretion. Heterozygous knockout of Kir6.2 ($Kir6.2^{+/-}$) or SUR1 ($SUR1^{+/-}$) decreases K_{ATP} channel activity and gives rise to hyperinsulinemia. Total knockout of Kir6.2 ($Kir6.2^{-/-}$) or SUR1 ($SUR1^{-/-}$) produces further enhancement of excitability and undersecretion in adult life. The position of hetE1506K and homE1506K mice at 2 (2mo) and 6 (6mo) months of age on this inverse U-shaped relationship is indicated.

Finally, our results suggest that some of the differences in secretory response previously reported for $SUR^{-/-}$ islets may (in part) reflect not only age and overnight culture but whether (17) or not (19) secretion was expressed relative to insulin content.

Summary. In conclusion, our data show that the homE1506K mouse provides a useful model of congenital hyperinsulinemia. Like heterozygous patients with this mutation, homE1506K mice show increased insulin secretion in early life but reduced secretion later in life. Our results show that, in the mouse, this is due to a reduction in insulin content, and not islet number or size, or β-cell area. If this finding translates to humans with the same mutation, it suggests that finding ways to preserve or enhance insulin content in later life might be a useful therapeutic strategy.

ACKNOWLEDGMENTS

This study was supported by the Wellcome Trust, the Royal Society, and the European Union (EuroDia LSHM-CT-2006-518153). F.M.A. is a Royal Society Research Professor.

No potential conflicts of interest relevant to this article were reported.

K.S. performed and analyzed insulin secretion and IPGTT experiments. M.T. performed and analyzed phenotyping experiments and statistics. M.I., M.F.B., and H.H. performed and analyzed phenotyping experiments. S.K. performed and analyzed calcium measurements. P.P. performed and analyzed electrophysiology experiments. C.L. performed and analyzed qtPCR experiments. N.Y. performed and analyzed Western blotting and statistics. S.M. performed and analyzed Western blotting. J.U. performed morphometric analysis. T.O. and M.L. planned the experiments. F.M.A. planned the experiments and wrote the manuscript. All authors read and approved the manuscript and contributed to the discussion. F.M.A., M.L., and T.O. are the guarantors of this work and, as such, had full access to all the data in the study and take responsibility for the integrity of the data and the accuracy of the data analysis.

The authors thank the animal house staff for taking care of the mice. The authors acknowledge the Genetic Engineering Service (Institut Clinique de la Souris, Illkirch-Graffenstaden, France) for the production of the knock-in mice.

REFERENCES

1. De León DD, Stanley CA. Mechanisms of disease: advances in diagnosis and treatment of hyperinsulinism in neonates. Nat Clin Pract Endocrinol Metab 2007;3:57–68
2. Hussain K, Cosgrove KE. From congenital hyperinsulinism to diabetes mellitus: the role of pancreatic beta-cell K_{ATP} channels. Pediatr Diabetes 2005;6:103–113
3. Thomas PM, Cote GJ, Wohllk N, et al. Mutations in the sulfonylurea receptor gene in familial persistent hyperinsulinemic hypoglycemia of infancy. Science 1995;268:426–429
4. Flanagan SE, Clauin S, Bellanné-Chantelot C, et al. Update of mutations in the genes encoding the pancreatic beta-cell $K_{(ATP)}$ channel subunits Kir6.2 (*KCNJ11*) and sulfonylurea receptor 1 (*ABCC8*) in diabetes mellitus and hyperinsulinism. Hum Mutat 2009;30:170–180
5. Ashcroft FM. The Walter B. Cannon Physiology in Perspective Lecture, 2007. ATP-sensitive K+ channels and disease: from molecule to malady. Am J Physiol Endocrinol Metab 2007;293:E880–E889

6. Remedi MS, Nichols CG. Hyperinsulinism and diabetes: genetic dissection of β-cell metabolism-excitation coupling in mice. Cell Metab 2009;10:442–453
7. Tucker SJ, Gribble FM, Zhao C, Trapp S, Ashcroft FM. Truncation of Kir6.2 produces ATP-sensitive K+ channels in the absence of the sulphonylurea receptor. Nature 1997;387:179–183
8. Nichols CG, Shyng SL, Nestorowicz A, et al. Adenosine diphosphate as an intracellular regulator of insulin secretion. Science 1996;272:1785–1787
9. Huopio H, Reimann F, Ashfield R, et al. Dominantly inherited hyperinsulinism caused by a mutation in the sulfonylurea receptor type 1. J Clin Invest 2000;106:897–906
10. Thornton PS, MacMullen C, Ganguly A, et al. Clinical and molecular characterization of a dominant form of congenital hyperinsulinism caused by a mutation in the high-affinity sulfonylurea receptor. Diabetes 2003;52:2403–2410
11. Lin YW, Bushman JD, Yan FF, et al. Destabilization of ATP-sensitive potassium channel activity by novel *KCNJ11* mutations identified in congenital hyperinsulinism. J Biol Chem 2008;283:9146–9156
12. Pinney SE, MacMullen C, Becker S, et al. Clinical characteristics and biochemical mechanisms of congenital hyperinsulinism associated with dominant K_{ATP} channel mutations. J Clin Invest 2008;118:2877–2886
13. Shemer R, Avnon Ziv C, Laiba E, et al. Relative expression of a dominant mutated *ABCC8* allele determines the clinical manifestation of congenital hyperinsulinism. Diabetes 2012;61:258–263
14. Huopio H, Otonkoski T, Vauhkonen I, Reimann F, Ashcroft FM, Laakso M. A new subtype of autosomal dominant diabetes attributable to a mutation in the gene for sulfonylurea receptor 1. Lancet 2003;361:301–307
15. Abdulhadi-Atwan M, Bushman J, Tornovsky-Babaey S, et al. Novel de novo mutation in sulfonylurea receptor 1 presenting as hyperinsulinism in infancy followed by overt diabetes in early adolescence. Diabetes 2008;57:1935–1940
16. Männikkö R, Flanagan SE, Sim X, et al. Mutations of the same conserved glutamate residue in NBD2 of the sulfonylurea receptor 1 subunit of the KATP channel can result in either hyperinsulinism or neonatal diabetes. Diabetes 2011;60:1813–1822
17. Seghers V, Nakazaki M, DeMayo F, Aguilar-Bryan L, Bryan J. Sur1 knockout mice. A model for $K_{(ATP)}$ channel-independent regulation of insulin secretion. J Biol Chem 2000;275:9270–9277
18. Shiota C, Larsson O, Shelton KD, et al. Sulfonylurea receptor type 1 knockout mice have intact feeding-stimulated insulin secretion despite marked impairment in their response to glucose. J Biol Chem 2002;277:37176–37183
19. Szollosi A, Nenquin M, Henquin JC. Pharmacological stimulation and inhibition of insulin secretion in mouse islets lacking ATP-sensitive K^+ channels. Br J Pharmacol 2010;159:669–677
20. Nenquin M, Szollosi A, Aguilar-Bryan L, Bryan J, Henquin JC. Both triggering and amplifying pathways contribute to fuel-induced insulin secretion in the absence of sulfonylurea receptor-1 in pancreatic beta-cells. J Biol Chem 2004;279:32316–32324
21. Clark RH, McTaggart JS, Webster R, et al. Muscle dysfunction caused by a K_{ATP} channel mutation in neonatal diabetes is neuronal in origin. Science 2010;329:458–461
22. Pfaffl MW. A new mathematical model for relative quantification in real-time RT-PCR. Nucleic Acids Res 2001;29:e45
23. Girard CA, Wunderlich FT, Shimomura K, et al. Expression of an activating mutation in the gene encoding the KATP channel subunit Kir6.2 in mouse pancreatic beta cells recapitulates neonatal diabetes. J Clin Invest 2009;119:80–90
24. Henquin JC, Nenquin M, Sempoux C, et al. In vitro insulin secretion by pancreatic tissue from infants with diazoxide-resistant congenital hyperinsulinism deviates from model predictions. J Clin Invest 2011;121:3932–3942
25. Gribble FM, Tucker SJ, Haug T, Ashcroft FM. MgATP activates the beta cell KATP channel by interaction with its SUR1 subunit. Proc Natl Acad Sci USA 1998;95:7185–7190
26. Henquin JC. The dual control of insulin secretion by glucose involves triggering and amplifying pathways in β-cells. Diabetes Res Clin Pract 2011;93(Suppl. 1):S27–S31
27. Nakazaki M, Crane A, Hu M, et al. cAMP-activated protein kinase-independent potentiation of insulin secretion by cAMP is impaired in SUR1 null islets. Diabetes 2002;51:3440–3449
28. Zhang CL, Katoh M, Shibasaki T, et al. The cAMP sensor Epac2 is a direct target of antidiabetic sulfonylurea drugs. Science 2009;325:607–610
29. Marshak S, Leibowitz G, Bertuzzi F, et al. Impaired beta-cell functions induced by chronic exposure of cultured human pancreatic islets to high glucose. Diabetes 1999;48:1230–1236
30. Melloul D, Marshak S, Cerasi E. Regulation of insulin gene transcription. Diabetologia 2002;45:309–326
31. Cnop M, Foufelle F, Velloso LA. Endoplasmic reticulum stress, obesity and diabetes. Trends Mol Med 2012;18:59–68
32. Takahashi A, Nagashima K, Hamasaki A, et al. Sulfonylurea and glinide reduce insulin content, functional expression of $K_{(ATP)}$ channels, and accelerate apoptotic beta-cell death in the chronic phase. Diabetes Res Clin Pract 2007;77:343–350
33. Miki T, Nagashima K, Tashiro F, et al. Defective insulin secretion and enhanced insulin action in K_{ATP} channel-deficient mice. Proc Natl Acad Sci USA 1998;95:10402–10406
34. Hugill A, Shimomura K, Ashcroft FM, Cox RD. A mutation in KCNJ11 causing human hyperinsulinism (Y12X) results in a glucose-intolerant phenotype in the mouse. Diabetologia 2010;53:2352–2356
35. Remedi MS, Rocheleau JV, Tong A, et al. Hyperinsulinism in mice with heterozygous loss of $K_{(ATP)}$ channels. Diabetologia 2006;49:2368–2378
36. Remedi MS, Koster JC, Markova K, et al. Diet-induced glucose intolerance in mice with decreased beta-cell ATP-sensitive K^+ channels. Diabetes 2004;53:3159–3167